INL/CON-07-13340
PREPRINT

A New Single-Crystal Filtered Thermal Neutron Source for Neutron Capture Therapy Research at the University of Missouri

International Conference on Reactor Physics, Nuclear Power: A Sustainable Resource

John Brockman
David W. Nigg
M. Frederick Hawthorne
Charles McKibben

September 2008

International Conference on Reactor Physics, Nuclear Power: A Sustainable Resource
Casino-Kursaal Conference Center, Interlaken, Switzerland, September 14-19, 2008

A new single-crystal filtered thermal neutron source for neutron capture therapy research at the University of Missouri

John Brockman[a], David W. Nigg[b*], M. Frederick Hawthorne[a], Charles McKibben[a]

[a] *University of Missouri, Columbia, MO USA*
[b] *Idaho National Laboratory, Idaho Falls ID USA*

Abstract

Parameter studies, design calculations and initial neutronic performance measurements have been completed for a new thermal neutron beamline to be used for neutron capture therapy cell and small-animal radiobiology studies at the University of Missouri Research Reactor. The beamline features the use of single-crystal silicon and bismuth sections for neutron filtering and for reduction of incident gamma radiation. The calculated and measured thermal neutron flux produced at the irradiation location is on the order of 9.5×10^8 neutrons/cm^2-s, with a measured cadmium ratio (Au foils) of 105, indicating a well-thermalized spectrum.

1. Introduction

Neutron Capture Therapy (NCT) is a binary cancer treatment modality that utilizes a neutron source coupled with a suitable nuclide to induce radiation damage in a tumor. In current practice the neutron capture nuclide is ^{10}B and therefore the therapy is referred to as BNCT. The ^{10}B is incorporated in a targeting agent molecular structure that provides in-vivo chemical stability and targets specific cell or tumor types. Following administration of the BNCT agent and subsequent uptake into the malignant tissue the treatment volume is exposed to a field of thermal neutrons. The neutrons interact with ^{10}B, producing an alpha particle and lithium ion. These highly-energetic (~2.35 MeV total energy) charged particles deposit their energy within a volume that is comparable to the size of the malignant cell, leading to a high probability of cell inactivation by direct DNA damage. In one sense, NCT can also be regarded as a high linear energy transfer (LET) targeted radionuclide therapy where the radionuclide can be switched on and off. BNCT treatment thus offers the possibility of highly selective destruction of malignant tissue while sparing healthy, neighboring tissue.

*Corresponding author, dwn@inel.gov , Tel 208-526-7627, Fax 208-526-2930

Some limited initial human trials of BNCT treatment of brain tumors were conducted in the U.S. in the 1950s and early 1960s. In September 1994 two sets of "Second Generation" human BNCT clinical trials for glioblastoma multiforme (a highly-malignant primary brain tumor) and for melanoma of the extremities were undertaken in the U.S. These Phase I studies were independently conducted at the Massachusetts Institute of Technology (MIT) and at Brookhaven National Laboratory (BNL) in New York. Results of the recent U.S. BNCT trials and similar trials currently ongoing at research centers in Europe, Japan, and Argentina show positive trends but much work remains. Observations based on the limited available data indicate that treatment efficacy for the tumors studied appears to be at least comparable to that of the best alternative standard treatments. In addition, key patient safety issues have been successfully addressed in the modern protocols. As is often the case with new cancer therapies, the clinical results obtained so far with BNCT are thus not dramatic, but there is clearly significant promise to the concept.

The more recent (post-1994) BNCT trials differ from the earlier trials largely because of the availability of significantly improved neutron sources and implementation of much more accurate computational and experimental dosimetry, including the required analytical chemistry. In contrast, there have been essentially no improvements in the boron containing targeting agents approved for human applications in the last 30 years. The available approved BNCT compounds, while offering some attractive features, are still not optimal for the treatment of tumors of interest (Hawthorne and Lee, 2003).

It has thus become apparent that the next quantum leap in clinical BNCT efficacy must come from improved alternatives to the current approved boron targeting agents. In fact, it has been demonstrated that improved BNCT agents are essential to take full advantage of recent improvements in neutron source technology (Wheeler et al., 1999). Furthermore, it will be useful to study applications to a broader spectrum of tumor types, even with current agents (e.g. Kankaanranta et al., 2007; Dagrosa et al., 2007). And in fact, several highly-promising new boron agents that may offer improved biochemical properties *and* that are potentially capable of treating a wider variety of tumor types are available (Hawthorne and Lee, 2003) but for various reasons they have not been systematically evaluated in small- and large-animal models to a sufficient degree to permit human trials, and some have not been evaluated at all.

In this context, the University of Missouri (MU) Institute for Nano and Molecular Medicine, the Idaho National Laboratory (INL) and the University of Missouri Research Reactor (MURR) are collaborating in a new research initiative to further the development of improved BNCT agents and treatment protocols, for a broader array of tumor types. Key initial agents and delivery mechanisms to be investigated over the course of this multiyear planned effort include boron-containing unilamellar liposomes (ULL) delivering amphiphilic alkyl-substituted nidocarborane anion salt (MAC) as well as the sodium salt of a hydrophilic $[B_{20}H_{17}NH_3^{3-}]$ ion (TAC). The first step of this effort has involved the design and construction of a new thermal neutron beam irradiation facility for cell and small-animal radiobiological research at the MURR. In this paper we present the beamline design with the results of pertinent neutronic design calculations as well as initial neutronic performance measurements.

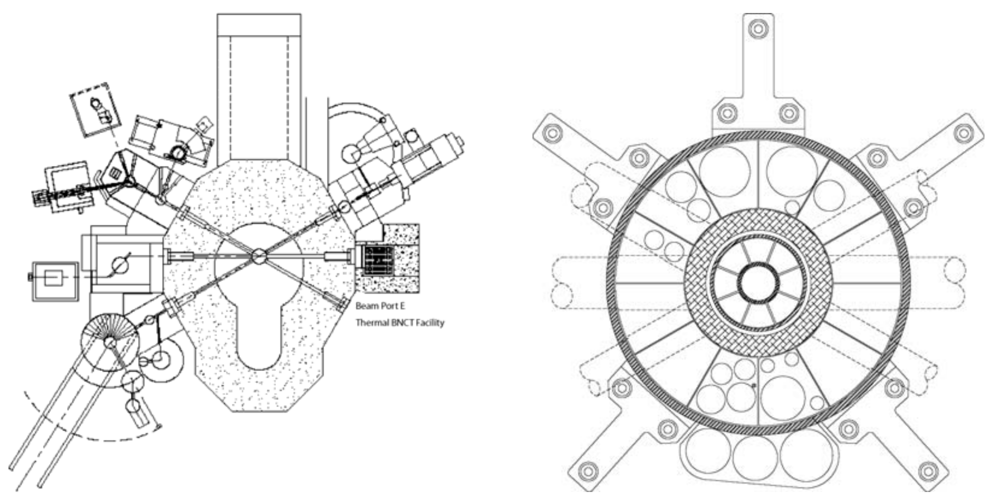

Figure 1. Top view of MURR reactor, shielding, and beamlines (L), and core detail (R) showing fuel annulus, beryllium reflector, and graphite reflector. Beamline E extends from the core horizontally to the right in this view.

2. Facility Description

The MURR reactor (Figure 1) features a compact light-water cooled and moderated fully-enriched annular core composed of eight plate-fuel elements with a maximum licensed power level of 10 MW. The outer radius of the core is approximately 14.9 cm, with an active height of 60.96 cm. The core is surrounded by a beryllium reflector, followed by a graphite reflector. Details of the new beamline design are shown in Figure 2. It will be located in an existing 15.24 cm (6”) diameter MURR beam tube, referred to as Beamline E, which extends from the outer surface of the beryllium reflector, through the graphite reflector, and out through the biological shield wall as shown in the figures. Key features of the new beamline include the use of a single-crystal silicon neutron filtering section followed by a single-crystal bismuth section in a manner similar to that reported by Kim et al. (2007), but without cryogenic cooling of the crystals. The irradiation location is just downstream of the bismuth filter section, at a distance of approximately 3.95 meters from the central axis of the reactor. A shielding enclosure surrounds the exit port of the beamline as shown. A hydraulic lift inside this shield enclosure enables the remote placement of samples or animals being irradiated.

The single-crystal silicon section in the beamline provides the bulk of the spectral filtering, while the bismuth section provides some final neutron filtering along with its key function of reducing the incident gamma component in the beam. When the beam is not in use, the bismuth filter section rotates out of the beamline and is replaced by a Pb, steel, boral and polyethylene laminated shutter.

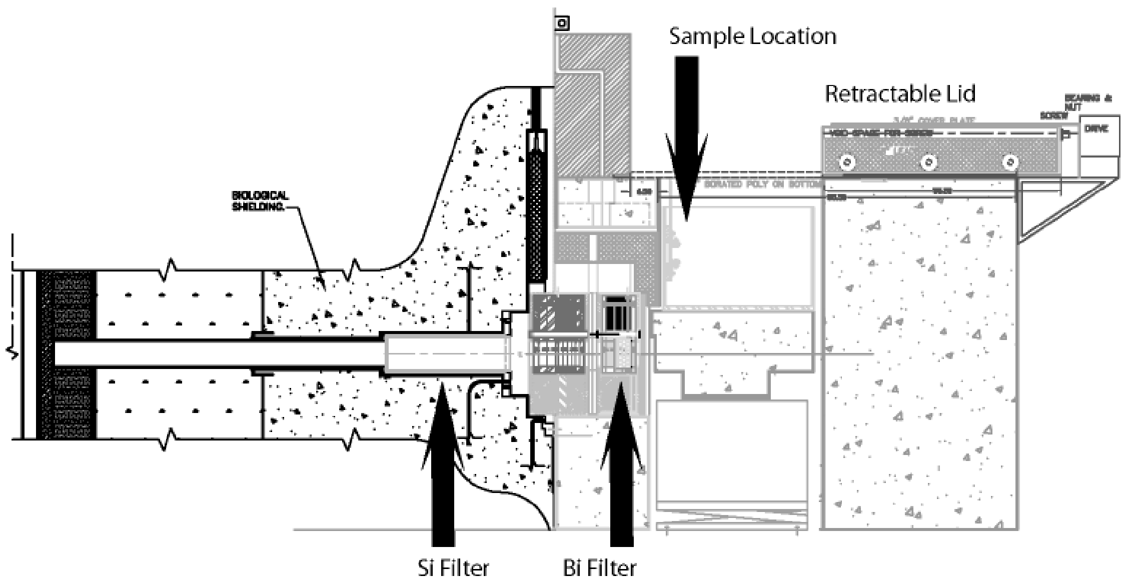

Figure 2. MURR thermal beamline design detail, shown in a closed configuration to allow access to samples.

In order to achieve the required neutron flux at the irradiation point it was critical to obtain filter materials of sufficient quality. High purity, single-crystal silicon is readily available in the commercial market. We purchased 75 cm of high purity silicon crystal from Bollen Semiconductor (Ohio, USA) in 5 cylindrical segments 19.5 cm in diameter and 15 cm in thickness, all cut from the same crystal. In order to achieve more flexibility for adjusting the total filter length in the beamline, one 15-cm segment was further cut into 5 cm and 10 cm thick segments. In contrast to the situation with silicon, single bismuth crystals of sufficient size and quality are difficult to obtain. These had to be especially grown for our use and it was unknown how crystal imperfections would influence neutron transmission, so the development of a suitable specification for the bismuth crystal was problematic. Ultimately we commissioned the fabrication of two bismuth crystals, 8 cm in thickness and approximately 18 cm in diameter by two different manufacturers. We also purchased a 10 cm thick bismuth crystal in the event that more gamma ray shielding was necessary, or if the thermal neutron transmission was higher then expected, which would permit additional neutron filtering to further improve the beam quality. The first 8 cm bismuth crystal (1) was manufactured by Monocrystals Inc. (Ohio, USA), the second 8 cm crystal (2), and the 10 cm crystal (3), were manufactured by the Polish Institute of Atomic Energy (Otwock-Swierk, Poland). None of the bismuth filters were actually monolithic single crystals. Upon visual examination they appeared to be composites of several crystals (Figure 3). While no formal test was undertaken to characterize the bismuth crystals, a visual inspection indicated that Crystals 2 and 3 had fewer grains than Crystal 1. As noted above, it was unknown whether this increased granularity would affect the neutron transmission to any significant extent.

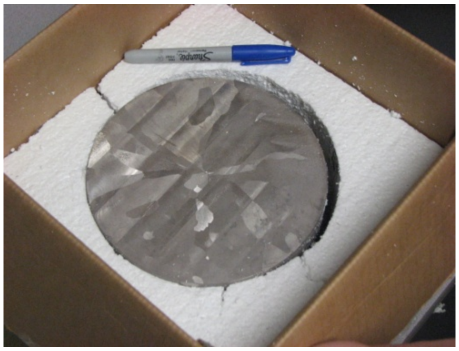

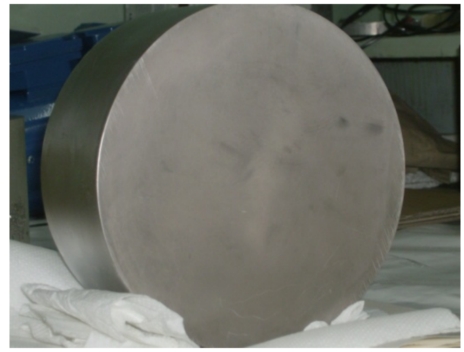

Figure 3. Bismuth crystals manufactured by Monocrystals (Left) and by the Polish Institute of Atomic Energy (Right). Both are 8 cm in thickness.

3. Computational Methods and Models

Independent deterministic and stochastic models of the coupled reactor core and beamline were developed using the DORT (Rhoades et al., 1993) two-dimensional radiation transport code, with a highly forward-biased angular quadrature set consisting of 315 angular directions, and the MCNP-5 Monte Carlo code (Breismeister, 2000), respectively. The BUGLE-80 47-neutron, 20-gamma group cross section library (Roussin, 1980) was employed for the DORT computations, in keeping with previous practice for analysis of a number of other NCT neutron facilities worldwide. Modeling of the MURR with the two-dimensional cylindrical geometry option in DORT required a vertically-oriented model for the core, coupled at the outer boundary of the bismuth reflector to a separate, horizontal, model for the beamline. ENDF/B Version 6.8 cross section libraries were used with MCNP, except for two specialized cross section sets for the single-crystal bismuth and silicon filters in the MCNP calculations that were provided to MU and INL for this study by the Korean Atomic Energy Research Institute (Lee, 2007). These cross section sets were prepared (Kim et al., 2007) according to models described by Freund (1983). In the case of the DORT model, the thermal (Groups 46 and 47) scattering cross sections for amorphous bismuth and silicon in the BUGLE-80 library were adjusted to account for the single-crystal form of these materials using modified thermal cross sections computed by MCNP with the single-crystal libraries noted above. The adjusted cross sections were obtained by flux-volume weighting the MCNP reaction rates and fluxes in the thermal neutron energy range in the filter regions and then dividing the former by the latter to obtain effective 2-group (0 – 0.1 eV and 0.1 to 0.414 eV) thermal cross sections that reflect the reduction in thermal neutron scattering when the material is in single-crystal form. The capture cross sections were unchanged.

A number of parameter studies were conducted with DORT and, independently, with MCNP, varying the thicknesses of the silicon and bismuth filter sections to find an optimum that maximized the thermal neutron flux while maintaining the fast-neutron and gamma components of the beam within acceptable ranges. Both the DORT and the MCNP beamline optimization computations led to the conclusion that the silicon filtering section should be approximately 50-55 cm in thickness along the beamline, while the bismuth section should be 8 cm in thickness.

Neutron spectra at the irradiation location, computed using the DORT discrete-ordinates model, are shown in Figure 4. The spectral shapes computed by MCNP were consistent with the DORT results shown, within the MCNP statistical uncertainties. Results are presented in Figure 4 for the unfiltered beamline, for the beamline with 50 cm of silicon only, and for the fully-filtered Si(50cm)/Bi(8cm) beamline. Modification of the spectrum to reduce the above-thermal component relative to the thermal component from one case to the next is apparent. The total calculated thermal neutron flux (0 – 0.414 eV) delivered to the irradiation location by the fully-filtered beam (Si/Bi) was approximately 9.6×10^{8} neutrons/cm^2-s with an estimated uncertainty of approximately 10% based on previous experience at the INL with this type of computation for other BNCT neutron beams worldwide. The DORT calculations yielded an epithermal and fast-neutron kerma for the beam of approximately 1.2×10^{-11} cGy-cm^2, and an incident gamma kerma of approximately 4.0×10^{-11} cGy-cm^2. These results are consistent with typical design goals for this type of beam.

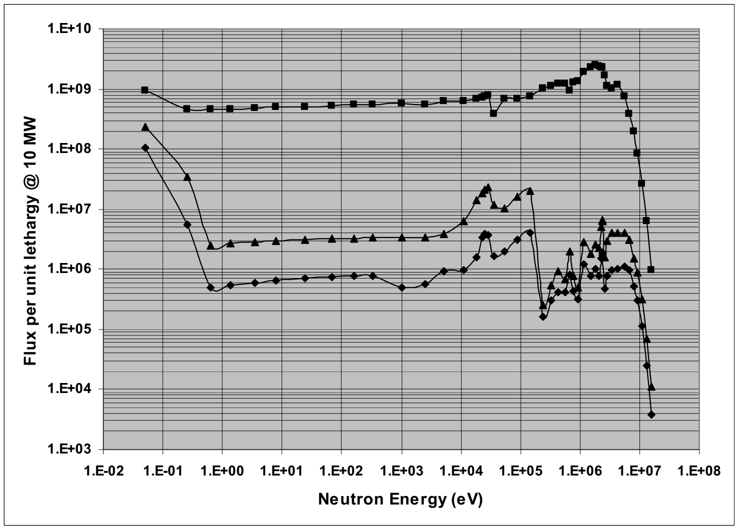

Figure 4. Computed unfiltered (■), silicon-filtered (▲), and Si+Bi filtered (♦) neutron spectra at the irradiation location for the baseline MURR thermal beamline design**.** Computations were performed with the DORT discrete-ordinates code with adjusted single-crystal silicon and bismuth cross sections.

4. Preliminary Measurements and Results

Basic beam performance measurements for an initial configuration of the beamline, prior to installing the final rotating shutter mechanism and beamstop shielding have been performed. These initial measurements were focused on quantifying the thermal neutron flux intensity and the approximate spectral quality. They were conducted using gold foils with and without cadmium covers as well as with flux wires composed of natural copper alloyed with 1.55% gold by weight. The gold foils were nominally 0.0254 mm (0.001") in thickness and 12.7 mm (0.5") in diameter, with masses of approximately 60 mg. The flux wires were 1 mm in diameter and approximately 10 mm in length, each with a mass of approximately 70 mg. Some scoping measurements to estimate the gamma dose rate at the irradiation location were also performed using Landauer TLD-100 dosimeters. The neutronics measurements reported here have provided key performance data needed to finalize the beamline component design and to complete the construction.

Measurements were conducted for each of the following beamline configurations:

- Open (voided) beamline.
- Each of the two different bismuth filters, 8 cm in thickness, and no silicon filter.
- The 10-cm bismuth filter and no silicon filter.
- Silicon filter, 50 cm in length, and no bismuth.
- Silicon filter, 50 cm in length, followed by the second 8-cm (Polish) bismuth filter.

The gold foils and copper wires were mounted on polymethyl methacrylate (PMMA) cards for irradiation in the beam as shown in Figure 5. Each irradiation card carried a gold foil, a Cd covered gold foil, or a TLD-100 mounted in the center of a hole cut into the card, along with two Cu/Au wires placed side by side and located 35 mm above the hole. Each measurement was repeated, resulting in a total of six irradiations for each beamline configuration of interest, with irradiation of a total of 2 TLD-100 gamma monitors, 2 bare Au foils, 2 Cd covered Au foils, and 12 Cu/Au wires in each case. The irradiation cards were attached to a 1 m aluminum rod for insertion into the irradiation position from above. The insertion rod was designed to reproducibly place a foil in the center of the beamline at the approximate axial location of the irradiation position in the planned final configuration. The irradiation times varied from 5 minutes in the voided beam configuration to 10 minutes in the silicon and bismuth filtered beams.

After irradiation, the activities of the foils and wires were measured using an ORTEC high-purity germanium detector calibrated using a NIST traceable mixed gamma source purchased from Analytics Inc. An absolute efficiency calibration of the detector was developed for distances of 7.62 cm, 12.7 cm, and 25.4 cm from the detector face.

A detector position was chosen for each set of wires and foils that minimized detector dead time while generating sufficient counts in a reasonable time. The detector dead time for every measurement was held to less than 2%. The gold foils were counted until there were at least 10,000 net counts in the 411 keV peak. The Cu/Au wires were counted until there were 1500 net counts in the peak at 411 keV from the ^{198}Au decay and 5000 net counts in the 511 keV positron annihilation peak from the decay of ^{64}Cu. Corresponding saturation activities per atom were computed for each foil or wire in the usual manner, using standard gamma intensity values of 0.96 gammas per decay for ^{198}Au and 0.34 gammas per decay for ^{64}Cu. (The positron decay branching ratio for ^{64}Cu is approximately 17% but there are two 0.511 MeV gammas produced per decay). The cadmium ratio for the gold foils was calculated in each case by dividing the average saturation activity per atom of Au measured for the two bare gold foils by the average saturation activity per atom of Au measured for the two cadmium covered gold foils.

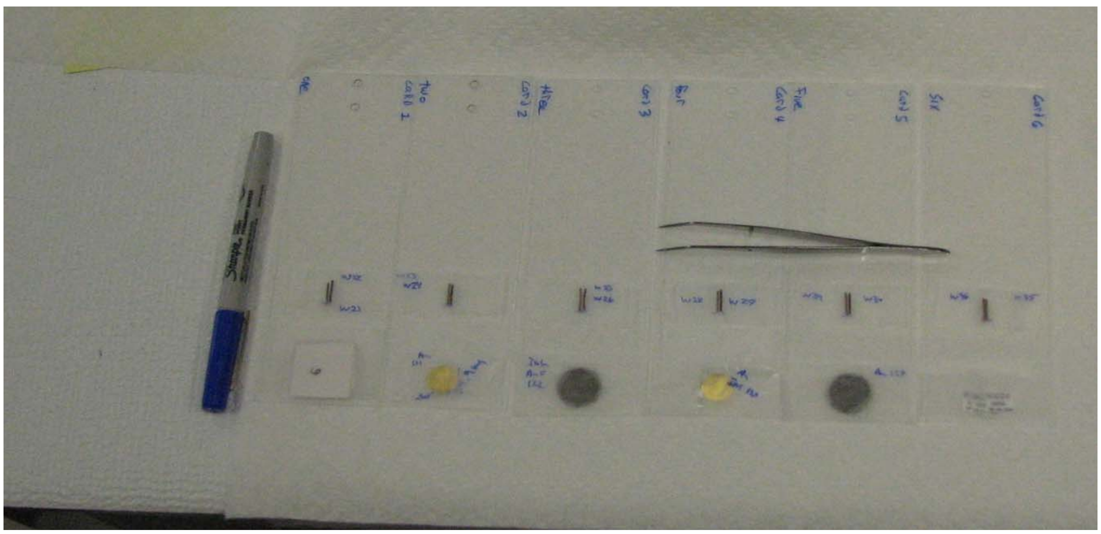

Figure 5. Typical mounting of gold foils, Cd covered gold foils, and Cu/Au wires on PMMA cards for a given series of irradiations in the beam.

The results of the preliminary measurements for the four primary beamline configurations of interest (open, 8 cm of bismuth and no silicon, 50 cm of silicon and no bismuth, and 50 cm of silicon followed by 8 cm of bismuth) are listed in Table 1. The "measured" thermal flux values given in Table 1 were obtained by dividing the difference between the bare and cadmium-covered foil activities by a computed (MCNP) effective average thermal (0-0.414 eV) cross section for the bare foils (91.3 b ± 3%). The voided case resulted in a measured thermal flux of 9.8E+9 n/cm^2·s. The bismuth crystal performance measurement results were essentially the same for the two 8 cm bismuth crystals, indicating that differences in the number of visible crystal imperfections observed in these crystals did not significantly affect the thermal neutron transmission. The second 8 cm crystal, manufactured by the Polish Institute of Atomic Energy, was selected for use in the final beamline. It is the measured results for this crystal that are shown in Table 1. The silicon filter increased the cadmium ratio from 3.1 in the voided beamline case to 65.3 indicating that it is effectively removing epithermal neutrons while transmitting thermal neutrons. The final test configuration featured the 50 cm silicon filter followed the Polish 8 cm bismuth filter as noted. The measured thermal flux in this case was 9.40E+8 n/cm^2·s with a Cd ratio 105. The measurements thus indicate that there is sufficient thermal neutron flux available for small animal BNCT studies.

The statistical uncertainties associated with the saturation activities shown in Table 1 are approximately 2% (1σ), including both the counting statistics for the foil being measured as well as the uncertainty associated with the detector calibration. In addition, based on the observed reproducibility of the foil measurements for each beamline configuration, it is estimated that there is an additional systematic uncertainty of approximately 3% associated with the saturation activities in Table 1. This is probably due largely to positioning uncertainty of the foils in the beam and possibly also to the effect of small reactor power drifts during a given irradiation.

The measured cadmium ratios for the various configurations are very consistent with expectations from the DORT and MCNP computations and show the anticipated trend toward greater thermalization of the beam as filter components are added. The ratios of gold activity to copper activity in the flux wires for each configuration confirm the spectral trends shown by the foil data. This ratio approaches a theoretical minimum of approximately 22 (i.e. the corresponding thermal cross section ratio) as the beam is increasingly thermalized by the various filter combinations.

Comparison of the calculated neutron flux values to the measured results is quite satisfactory at this point in the beam development although it appears that the computational procedures and data may tend to overpredict the thermal neutron transmission through the bismuth filters and underpredict the thermal neutron transmission through the silicon filter, with a somewhat compensatory effect for the two filters together.

The gamma dose measurements using the Landauer TLD-100 dosimeters were strongly correlated with the neutron flux with a calculated R^2 value of 0.98. This correlation is not unexpected since much of the incident gamma is due to prompt gammas produced by thermal neutron capture in and near the beamline. However, part of it could also be caused by the close proximity of the beam stop to the measurement location in these preliminary runs as compared to the planned final configuration, or by undue sensitivity of the LiF dosimeters to thermal neutrons. Thus the preliminary gamma measurements were viewed to be of limited utility, and are not reported here.

Table 1. Preliminary performance results: Voided and filtered beams for the thermal BNCT facility at MURR

	Voided Beamline	8 cm Bi Crystal	50 cm Si Crystal	50 cm Si + 8 cm Bi
Saturation Activity, Bare Gold Foil (decays/atom-s)	1.31×10^{-12} (5%)	3.82×10^{-13} (5%)	2.38×10^{-13} (5%)	8.67×10^{-14} (5%)
Saturation Activity , Cd Gold Foil (decays/atom-s)	4.11×10^{-13} (5%)	7.49×10^{-14} (5%)	3.64×10^{-15} (5%)	8.21×10^{-16} (5%)
Difference in Saturation Activity (decays/atom-s)	8.95×10^{-13} (8%)	3.07×10^{-13} (5%)	2.34×10^{-13} (5%)	8.59×10^{-14} (5%)
Measured Thermal Flux (n/cm^2-s)	9.80×10^{9} (11%)	3.36×10^{9} (8%)	2.56×10^{9} (8%)	9.40×10^{8} (8%)
Calculated Thermal Flux from DORT (n/cm^2-s)	9.38×10^{9} (10%)	3.81×10^{9} (10%)	2.22×10^{9} (10%)	9.62×10^{8} (10%)
Cadmium Ratio	3.18 (7%)	5.10 (7%)	65.3 (7%)	105.5 (7%)
Wire saturation activity ratio (Au/Cu)	36.4	28.4	22.4	22.4

Note: Reactor power is 10 MW. Uncertainties, discussed in the text, are shown in parentheses.

5. Conclusions and Future Work

Parameter studies, design calculations and initial performance measurements have been completed for a new thermal neutron beamline for neutron capture therapy cell and small-animal radiobiology studies at the University of Missouri Research Reactor. Results indicate that typical single-fraction irradiations to the required total accumulated dose for clinical relevance (6-10 Gy) can be conducted in an hour or less, depending on the tissue boron content, which is typically in the range of 20-100 parts per million by weight. Additional computational work will include refinement of the computational models as final construction is completed, and performance of some confirmatory computations using new single-crystal cross section data sets developed by Hawari et al. (2006).

Once the final beam shutter and beamstop shielding have been installed, a much more comprehensive set of activation measurements will be conducted to characterize the neutronic performance of the final system. Measurements will be conducted using foil packages composed of: 1) bare gold and manganese, 2) cadmium-covered gold, indium, tungsten, cobalt, manganese, copper, and possibly scandium and, 3) indium and nickel enclosed in a boron-10 sphere with a wall thickness of approximately 1 cm. This will provide up to 11 linearly-independent spectral response functions covering the energy range from thermal to about 2 MeV. The neutron spectrum will be unfolded using various methods, including standard adjustment techniques as well as an overdetermined least-squares fitting technique adapted by INL specifically for NCT purposes (Nigg, et al., 2000).

Additional measurements useful for estimating the spatial distribution of the thermal and above-thermal neutron flux at various locations on the surface of, and within, a standard cylindrical Lucite phantom (12.7 cm diameter, 18.1 cm height) and a small-animal phantom will also be performed using the activation of the copper-gold flux wires described previously. Finally, the incident gamma component of the MURR neutron source will be measured using a set of FarWest^{TM} paired ion chambers, in keeping with the recommendations of the International BNCT Dosimetry Exchange (Järvinen and Voorbrack, 2003).

6. References

Breismeister, JF, 1999. "MCNP – A General Monte Carlo N-Particle Transport Code, Version 4C, LA-13709-M, Los Alamos National Laboratory, USA .

Dagrosa, M.A., et al.,2007. "Optimization of Boron Neutron Capture Therapy for the Treatment of Undifferentiated Thyroid Cancer, International Journal of Radiation Oncology, Biology, and Physics, **69**:1059-1066.

Freund, A.K., 1983. Cross Sections of Materials used as Neutron Monochromators and Filters, Nuclear Instruments and Methods, **243:**495-501.

Hawthorne M.F. and Lee, M.W., 2003. A Critical Assessment of Boron Target Compounds for Boron Neutron Capture Therapy, Journal of Neuro Oncology 62:33-45.

Hawari, A.I., et al., 2006. Accurate Simulation of Thermal Neutron Filter Effects in the Design of Research Reactor Beam Applications, Proceedings of the American Nuclear Society Topical Meeting on Reactor Physics, PHYSOR-2006, Vancouver, BC, Canada.

Järvinen, H., and Voorbraak, W.P., 2003. Recommendations for the Dosimetry of Boron Neutron Capture Therapy, Report 21425/03 55339/C, NRG Petten, The Netherlands.

Kankaanranta, L., et al.,2007. Boron Neutron Capture Therapy in the Treatment of Locally Reccurent Head and Neck Cancer, International Journal of Radiation Oncology, Biology, and Physics, **69**:475-482.

Kim, Myong-Seop et al., 2007. Development and characteristics of the HANARO neutron irradiation facility for applications in the boron neutron capture therapy field, Phys. Med. Biol. **52** 2553-2566

Lee, Byung-Chul, 2007. Korea Atomic Energy Research Institute, Private communication.

Nigg, DW et al., 2000. Modification of the University of Washington Neutron Radiotherapy Facility for Optimization Neutron-Capture-Enhanced Fast Neutron Therapy, Med. Phys. **27**:359-367 (2000).

Rhoades, WA, et. al., 1993. TORT-DORT: Two and Three-Dimensional Discrete-Ordinates Transport, Radiation Shielding Information Center, Oak Ridge National Laboratory, CCC-543.

Roussin, R.W., 1980. BUGLE-80 Coupled 47-Neutron, 20 Gamma-Ray P3 Cross Section

Library, DLC-75, Radiation Shielding Information Center, Oak Ridge National Laboratory, USA.

Wheeler, F.J, Nigg, D.W., et al., 1999. Boron Neutron Capture Therapy: Implications of Neutron Beam and Boron Compound Characteristics, Med. Phys. **26**:1237-1244.

Acknowledgements

This work was supported by the University of Missouri Institute for Nano and Molecular Medicine. Some in-kind material contributions were made by the US Department of Energy through the Idaho National Laboratory.